Bond-orbital model. II†

W. A. Harrison and S. Ciraci*
Applied Physics Department, Stanford University, Stanford, California 94305
(Received 8 April 1974)

The bond-orbital model is reformulated taking explicit account of the large overlap of two hybrids in the same bond rather than absorbing it in a pseudopotential. This gives a correction to the cohesive energy but other changes are absorbed in the V_1, V_2, and V_3 for each material. These parameters are reevaluated taking band calculations as the standard for V_1 (but using the atomic term values to scale from material to material) and taking the energy of the optical-absorption peak as the standard for V_2 and V_3 (but using the dielectric constant to scale from material to material). Using the new parameters we test the model by comparison of predictions with experiment (or accurate calculations) for various valence-band gaps, the pressure dependence of the dielectric constant, the macroscopic transverse charge, the piezoelectric constant, the photoelectric threshold, and the cohesive energy. Discrepancies in the cohesive energy are found to scale with a reasonable form for the interbond correlation energy, giving a semiempirical expression for the cohesive energy in terms of parameters of the bond-orbital model. The covalent energy is found in this study to scale with a kinetic energy (with the inverse square of the bond length) both under pressure and for variation from material to material.

I. INTRODUCTION

Many years ago Hall[1] proposed a crude linear-combination-of-atomic-orbitals (LCAO) model of the valence-band structure for diamond. Coulson, Redei, and Stocker[2] extended this to partially ionic solids and defined an ionicity parameter in terms of the model. Friedel and co-workers[3] adopted the same point of view in discussing a range of bonding properties and materials. In fact, the intuitive picture of a valence band composed of tight-binding combinations of bond orbitals, each composed of an even combination of s-p hybrids, is a part of the thinking of many solid state physicists and chemists. The total energy calculations of Watkins and Messmer[4] using extended Hückel theory are conceptually related to this, though they did not strip the model to its simplest form as did the others. Quite recently Lannoo and Decarpigny[5] in treating the transverse effective charge, attempted to graft the simple LCAO model onto the somewhat vaguer ionicity concept of Phillips[6] (which has its conceptual origin in pseudopotential theory) in order to obtain parameters from the measured dielectric constants. At the same time one of us[7] formulated a very specific model, which he called the bond-orbital model (BOM), out of this general intuitive background. This made specific the assumptions, made clear the relation between the bands and the bond orbitals, systematized the notation, incorporated the effects of metallization as well as those of ionicity, extended the application to a wide range of properties, and explicitly evaluated the dielectric constant in terms of the model. This last step allowed the conceptual and computational unification of this semiempirical approach to the understanding of tetrahedrally oriented and partially covalent solids. We will refer to that work[7] as I.

The purpose of the present paper is threefold. First we reformulate the model more carefully to allow a more precise definition of the parameters. Second we evaluate and tabulate these parameters for a large range of materials. Third we test the approach for many properties and systems; only one or two illustrative examples were carried out in I. The principal results of I are confirmed in this more careful formulation though the parameters change slightly in value. The form of the valence bands remains the same. The change in parameters scales the transfer term of e_T^* [the last term in Eq. (18) of I] by $\frac{2}{3}$. The form of the dielectric constant is reconfirmed and the variation of V_2 with bond length is found to be changed considerably. An additional term $-8SV_2$ is to be added to the cohesive energy [Eq. (31) of I] and correlation corrections are found to be large. These would also modify the considerations of structural stability given in I. These are changes in details and to a first approximation the scheme is the same with refined parameters.

II. REFORMULATION OF THE MODEL

One of our principal purposes here is to select material parameters for the bond-orbital model. It is clear that there is no "best" way to do this. First, a choice which fits one property exactly may do badly on others and a compromise is to be made. Second, and more important, a compromise must be made on the number of parameters used. In the original formulation we took a universal parameter γ (we took the value $\gamma^2 = 2$), relating dipole moments to polarities, though of course a much better fit to experiment can be

made if γ is allowed to vary from material to material, or even from row to row in the Periodic Table. We will here follow the procedure of allowing only the three energies V_1, V_2, and V_3 to vary from material to material and will seek compromises on the values for more universal parameters such as γ. We will be aided considerably in this by a more complete formulation of the model taking explicit account of the nonorthogonality of the hybrid orbitals rather than absorbing that nonorthogonality in a pseudopotential. This will be more rigorous, more accurate, and allow discussion of a wider range of properties without seriously complicating the model.

We again consider tetrahedrally coordinated atoms and construct four hybrids on each atom, denoted $|h^a\rangle$ on the anion and $|h^c\rangle$ on the cation. The hybrid energy on the anion

$$\epsilon^a = \langle h^a | H | h^a \rangle = \tfrac{1}{4}(\epsilon_s^a + 3\epsilon_p^a) \tag{1}$$

may differ from the corresponding energy ϵ^c on the cation. We write the difference

$$M_3 = \tfrac{1}{2}(\epsilon^c - \epsilon^a) . \tag{2}$$

We will shortly relate M_3 to the parameter V_3, which is to be obtained from the measured dielectric constant for each material.

There are matrix elements of the Hamiltonian between two hybrids on the same anion,

$$M_1^a = -\langle h^a | H | h^{a'} \rangle = \tfrac{1}{4}(\epsilon_p^a - \epsilon_s^a) , \tag{3}$$

and M_1^c between two hybrids on the same cation. We will in fact take V_1^a and V_1^c to be 0.8 times the value obtained from Eq. (3) using the term values of Herman and Skillman,[8] for reasons to be discussed.

There are also matrix elements of the Hamiltonian between two hybrids extending into the same bond:

$$M_2 = -\langle h^c | H | h^a \rangle . \tag{4}$$

These two hybrids are not orthogonal to each other and in fact the overlap

$$S = \langle h^c | h^a \rangle \tag{5}$$

is quite large. Our estimate[9] for silicon, based on atomic orbitals appropriate to the solid, was 0.5 and we will use that value for all materials in the analysis though it does not enter explicitly until we discuss cohesion. All other matrix elements of the Hamiltonian and all other overlaps are neglected (or absorbed in the parameters we have retained).

We now obtain bond orbitals

$$|b\rangle = u_a |h^a\rangle + u_c |h^c\rangle \tag{6}$$

by minimizing the bond energy

$$\epsilon_b = \langle b | H | b \rangle / \langle b | b \rangle \tag{7}$$

by variation of u_a and u_c. This yields

$$\epsilon_b = \frac{M_2 S - [M_2^2 S^2 + (1 - S^2)(M_2^2 + M_3^2)]^{1/2}}{(1 - S^2)} , \tag{8}$$

which would equal the earlier result $(M_2^2 + M_3^2)^{1/2}$ if S were equal to zero. We may now define our parameters. The *covalent energy* is written

$$V_2 = M_2/(1 - S^2). \tag{9}$$

The *polar energy* is written

$$V_3 = M_3/(1 - S^2)^{1/2} \tag{10}$$

and Eq. (8) becomes

$$\epsilon_b = V_2 S - (V_2^2 + V_3^2)^{1/2} . \tag{11}$$

The maximum energy, which we identify with the antibonding state, is similarly found to be $V_2 S + (V_2^2 + V_3^2)^{1/2}$. It is convenient to call half the difference the *bonding energy*,

$$(\epsilon_a - \epsilon_b)/2 = (V_2^2 + V_3^2)^{1/2} . \tag{12}$$

The variational calculation for the bonding state also yields the coefficients u_a and u_c:

$$u_a^2 = \frac{1}{2}\left(\frac{1 - S(1 - \alpha_p^2)^{1/2}}{1 - S^2} + \frac{\alpha_p}{(1 - S^2)^{1/2}}\right) , \tag{13}$$

$$u_c^2 = \frac{1}{2}\left(\frac{1 - S(1 - \alpha_p^2)^{1/2}}{1 - S^2} - \frac{\alpha_p}{(1 - S^2)^{1/2}}\right) , \tag{14}$$

which reduces to the earlier result for $S = 0$. Here α_p is the polarity defined again as

$$\alpha_p = V_3/(V_2^2 + V_3^2)^{1/2} . \tag{15}$$

Of central importance in the model is the dielectric constant and the dipole associated with a bond. We will, as before, consider an isolated bond in a field and discuss corrections afterward. The geometry is simple if we consider a bond in a [111] direction in a cubic crystal and apply a field in the x direction; then all four bond directions are equivalent. Then we add to the Hamiltonian of Eq. (7) a term $-e\mathcal{E}x$. Treating the two hybrids as symmetrically disposed and measuring x from the bond center we find a change

$$\Delta\langle b | H | b \rangle = (u_a^2 \langle h^a | x | h^a \rangle + u_c^2 \langle h^c | x | h^c \rangle)(-e)\,\mathcal{E} .$$

Defining γ' by

$$\langle h^a | x | h^a \rangle - \langle h^c | x | h^c \rangle = \gamma' a/4 , \tag{16}$$

we obtain

$$\langle b | (-e)\, x\mathcal{E} | b \rangle = (u_a^2 - u_c^2)\,\gamma'(-e)\,\mathcal{E}a/8. \tag{17}$$

Note γ' would be unity if the center of gravity of each hybrid were at the nucleus. We expect it to be less than 1. Equation (17) corresponds to a dipole, in the absence of the field, from the two electrons in the bond and a compensating proton

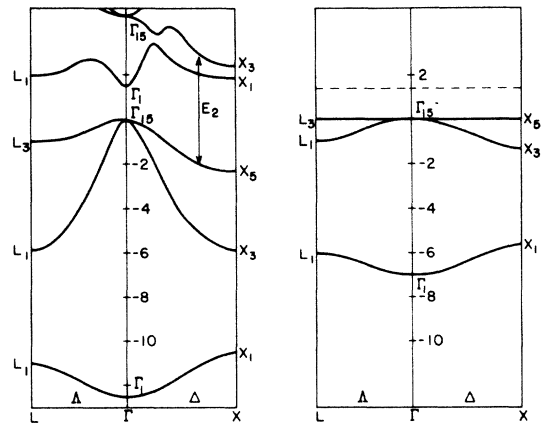

FIG. 1. Energy band structure of GaAs [F. Herman, R. L. Kortum, C. D. Kuglin, and J. P. Van Dyke, Methods Comput. Phys. 8, 193 (1968)] showing a transition which contributes to the absorption peak E_2. Also given are the symbols for the bands at symmetry points of interest. On the right is the corresponding valence band obtained in the BOM. All energies are in eV.

at each nucleus (so the system is neutral and the result is therefore independent of origin) of

$$P_x = -\gamma e \alpha_p a/4, \tag{18}$$

where we have defined the parameter γ to correspond to the earlier formulation:

$$\gamma = \gamma'/(1-S^2)^{1/2}. \tag{19}$$

We may follow the earlier calculation of the dielectric constant treating the system as independent polarizable bonds. Adding Eq. (17) to Eq. (7) has the effect of adding $\gamma e \mathcal{E} a/8$ to V_3. We may calculate the total energy to second order in $\mathcal{E}$ and identify the dielectric constant

$$\epsilon_0 = 1 + \gamma^2 \pi N e^2 d^2 V_2^2 / 3 (V_2^2 + V_3^2)^{3/2} \tag{20}$$

as before, where N is the density of electrons and d the bond length.

There are approximations in this approach that are most easily understood by calculating the response of the system to a long-wavelength potential $V_q \cos qx$ in perturbation theory. Again the unitary transformation from band states to bonding and antibonding orbitals can be made, now taking the energy difference between valence and conduction band as constant at $2(V_2^2 + V_3^2)^{1/2}$; this approximation is best for large band gaps. There are, however, matrix elements between bond orbitals and antibonding orbitals in adjacent bonds as well as those in the same bond which we have included here. These terms appear not to be so large, but add to the effective γ^2 of Eq. (20). In addition the local distortion of charge distribution can give local fields, different from the average, which could also modify the effective value of γ^2. It may well be true, on the other hand, that electron charge is transferred through the material without much local distortion so that these effects are small.

In any case, we adjust γ to experiment and all of these corrections are thereby absorbed. Comparison of a number of predictions of the model with experiment did not reveal any large trends with polarity or with metallicity among the Si, Ge, and Sn rows, though the carbon row appeared different. Thus we evaluate γ from experiment for C and for Si and use the Si value for the heavi-

TABLE I. Material parameters for the tetrahedral compounds. d is the bond length; V_1, V_2, and V_3 are the metallic, covalent, and polar energies, respectively; $(V_2^2+V_3^2)^{1/2}$ is the bonding energy; α_p is the polarity and α_m the metallicity.

Semiconductor	d (Å)	V_1 (eV)	V_2 (eV)	V_3 (eV)	$(V_2^2+V_3^2)^{1/2}$ (eV)	α_p	α_m
C	1.54	1.70	6.10	0	6.10	0	0.28
Si	2.35	1.41	2.20	0	2.20	0	0.64
Ge	2.44	1.60	2.15	0	2.15	0	0.74
α-Sn	2.80	1.33	1.76	0	1.76	0	0.76
SiC	1.88	1.62	3.66	1.54	3.97	0.39	0.41
BN	1.57	1.98	6.10	2.76	6.70	0.41	0.30
AlP	2.36	1.57	2.20	1.18	2.50	0.47	0.63
GaAs	2.45	1.74	2.15	1.21	2.47	0.50	0.70
InSb	2.81	1.41	1.76	1.04	2.04	0.51	0.69
BP	1.97	1.47	3.66	0[a]	3.66	0	0.40
BAs	2.07	1.53	3.62	0[a]	3.62	0	0.42
AlN	1.89	2.06	3.66	2.68	4.54	0.59	0.45
AlAs	2.43	1.65	2.18	1.06	2.42	0.44	0.68
AlSb	2.66	1.41	1.97	1.26	2.33	0.54	0.60
GaN	1.94	2.12	3.62	2.89	4.64	0.62	0.46
GaP	2.36	1.65	2.18	1.33	2.55	0.52	0.65
GaSb	2.65	1.45	1.94	0.94	2.16	0.44	0.67
InN	2.15	2.10	3.27	2.75	4.28	0.64	0.49
InP	2.54	1.62	1.97	1.41	2.42	0.58	0.67
InAs	2.61	1.70	1.94	1.22	2.30	0.53	0.74
BeO	1.65	2.61	6.10	5.07	7.93	0.64	0.33
MgS[b]	2.44	1.58	2.38	2.12	3.4	0.63	0.47
ZnSe	2.45	2.00	2.15	2.26	3.12	0.72	0.64
CdTe	2.81	1.61	1.76	2.08	2.72	0.76	0.59
BeS	2.10	1.59	3.66	0.78	3.75	0.21	0.43
BeSe	2.20	1.70	3.62	1.23	3.83	0.32	0.45
BeTe	2.40	1.26	3.27	0[a]	3.27	0	0.38
MgSe[b]	2.54	1.96	2.20	2.06	3.02	0.68	0.65
MgTe	2.76	1.55	1.97	1.79	2.66	0.67	0.59
ZnO	1.98	2.70	3.62	3.55	5.07	0.70	0.53
ZnS	2.34	1.96	2.18	2.32	3.18	0.73	0.62
ZnTe	2.64	1.61	1.94	1.99	2.78	0.72	0.58
CdS	2.53	1.96	1.97	2.37	3.08	0.77	0.64
CdSe	2.63	2.01	1.94	2.35	3.05	0.77	0.66
HgS[b]	2.53	1.95	2.19	2.51	3.33	0.75	0.59
HgSe[b]	2.64	2.01	2.00	2.45	3.16	0.77	0.64
HgTe[b]	2.76	1.60	1.84	2.18	2.85	0.76	0.56
CuBr	2.49	2.28	2.15	2.77	3.51	0.79	0.65
AgI	2.80	1.81	1.76	2.65	3.18	0.83	0.57
CuF	1.84	3.54	3.62	5.45	6.54	0.83	0.54
CuCl	2.34	2.28	2.18	2.47	3.29	0.75	0.69
CuI	2.62	1.80	1.94	2.44	3.12	0.78	0.58

[a]Our procedure led to small negative values of V_3^2 for these compounds.

[b]For these compounds we found no experimental ϵ_0 for the tetrahedrally coordinated form. We therefore used ionic radii to obtain d and Figs. 7 and 4 to obtain V_2 and V_3.

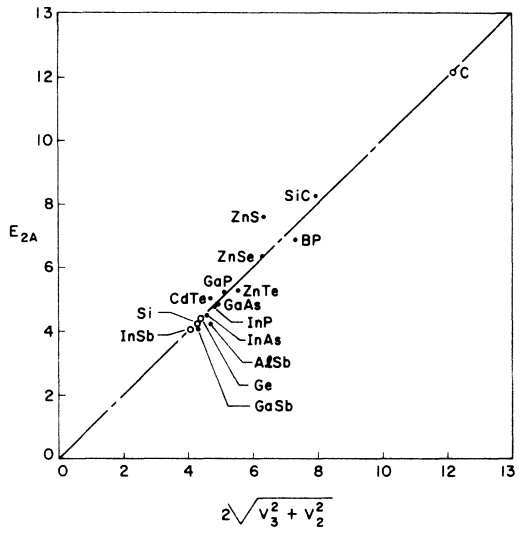

FIG. 2. Observed values of the absorption peak E_{2A} (Ref. 10) plotted against the BOM prediction. The empty points (C, Si, Ge, InSb) were fit but all others are independent predictions based ultimately upon the observed dielectric constant. All energies are in eV.

er elements.

The principal results of this formulation, once written in terms of V_1, V_2, V_3, and γ are essentially the same as in the earlier treatment though the difference, for nonzero S, in Eq. (11) is important and it is very desirable to have seen how the other effects of this large overlap can be absorbed in the model parameters.

III. CHOICE OF PARAMETERS

We tried a series of procedures for determining parameters before selecting the one which seemed to work best. We will not describe those we discarded, but only the one we used. Basically, the approach is to identify the energy of the principal optical-absorption peak E_2 with the bonding-antibonding energy gap. The kind of transition with which the peak is usually associated is indicated in the GaAs band structure shown in Fig. 1. This gives a value of the covalent energy V_2 for diamond of 6.1 eV, for silicon of 2.2 eV, and

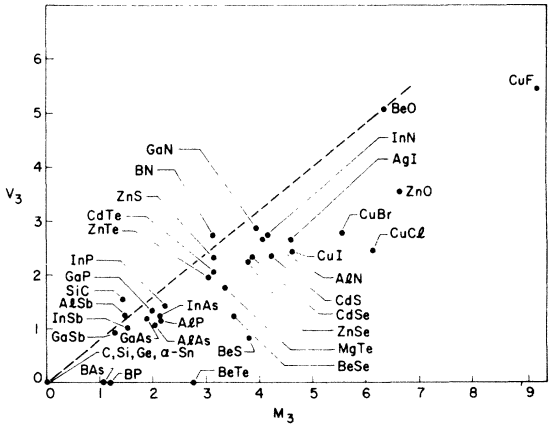

FIG. 3. Polar energies V_3 obtained from the measured dielectric constants [compiled, along with band lengths, by J. A. Van Vechten, Phys. Rev. 182, 891 (1969)] (and from covalent energies V_2 from the optical-absorption peaks), plotted against values obtained from Eqs. (1) and (2) and atomic term values (Ref. 8). The dashed line, slope 0.8, is suggested by consideration of the energy bands in Sec. III. Energies are in eV.

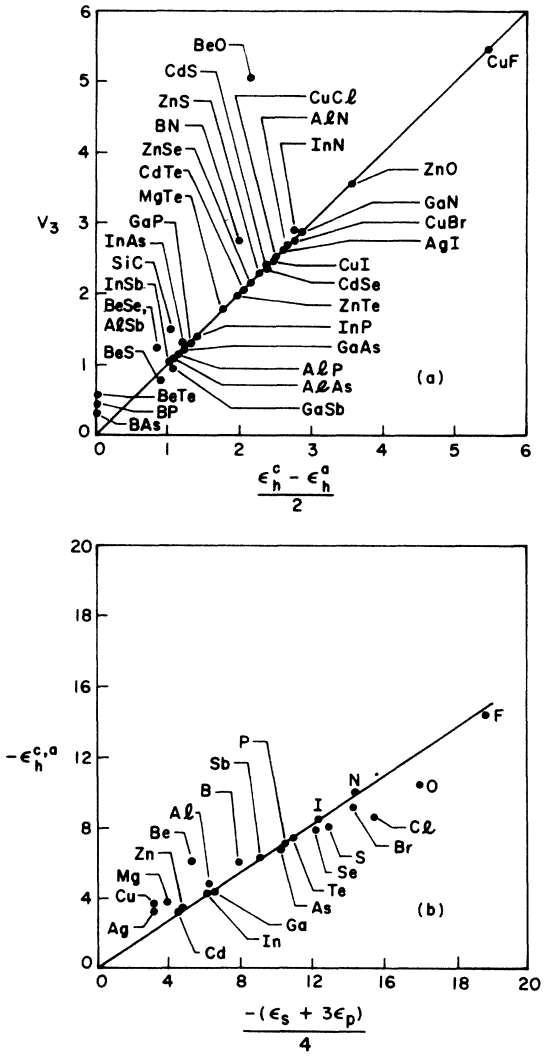

FIG. 4. (a) Polar energies V_3 (as in Fig. 3) plotted against values obtained from the hybrid energies of Table II. (b) Hybrid energies of Table II plotted against values from Eq. (1) and the atomic term values. Energies are in eV.

for germanium of 2.15 eV, using the table of Phillips[10] for the positions of these peaks. Unfortunately, the peaks are only known for a limited number of polar materials so we have used the dielectric-constant formula, and the assumption that V_2 depends only upon the row in the Periodic Table, to extend these results to the compounds and obtain the polar energy V_3; this seems preferable to using a different scheme on different materials and the method is tested by comparing predicted E_2 values with those which have been measured. Using these values of V_2 and the experimental dielectric constant of Eq. (20) we solve for γ and obtain 1.08 for diamond and 1.2 for silicon. We could proceed similarly to obtain a γ for germanium; however, we should recognize, as emphasized by Phillips,[6] that there are contributions to the dielectric constant from the polarizable core d states and that these corrections will enter the dielectric constant but not other properties. Thus we take the silicon value of γ for all materials below the carbon row in the Periodic Table and introduce a correction factor θ (i.e., we replace γ^2 by $\gamma^2\theta^2$) and obtain the value $\theta = 1.18$ for germanium using the measured dielectric constant. We do not have a value for the absorption peak E_2 for tin but we use the observed value for InSb, correcting for the polarity obtained from the respective dielectric constants. This leads to a value of $V_2 = 1.76$, and a value of $\theta = 1.41$ for the tin row. For any compound, both of whose components are in the same row of the Periodic Table, we take V_2, γ, and θ to be the same as that for the column-four element in that row. Then from Eq. (20) and the observed dielectric constant we obtain directly V_3. For skew compounds, consisting of elements from two rows, we take V_2 to be the geometric mean $(V_2^c V_2^a)^{1/2}$ of the values for the two rows, and take one factor of γ and one factor of θ from each. Then again from Eq. (20) and the measured dielectric constant we obtain directly V_3. The corresponding values of V_2 and V_3 are listed in Table I.

The determination of V_3 values was completely straightforward in all cases except BP and BAs. In both of those cases the dielectric constant corresponded to a bonding-antibonding gap slightly less than V_2; for these we have taken $V_3 = 0$. We suspect that this inconsistency arises from an inaccuracy of the model rather than of the experiment, but that it does reflect correctly a very small value of V_3 for these materials.

In obtaining these values we used the optical-absorption peak E_2 only for C, Si, Ge, and InSb. Having obtained V_2 and V_3 for other materials from the dielectric constants we may directly predict the absorption peaks for any other compound as a test of the scheme. The observed values, where they are known, are plotted against our calculated values in Fig. 2. The agreement is very good and strongly supports our choice of parameters.

We may compare the V_3 values we have obtained from those we would have obtained from the difference in hybrid energies based upon atomic term values. This comparison is made in Fig. 3. The correlation is good but the spread is sufficient to make it clear that the use of experimental dielectric constants is warranted. Indeed the spread comes principally from the use of *atomic* term values. We may choose hybrid energies which, by direct subtraction, give rather good values for the polar energy of the compound; i.e., $V_3 = (\epsilon_h^c - \epsilon_h^a)/2$. Such a set of hybrid energies is given in Table II. The extent to which we have succeeded in fitting the entire set of polar energies with a single set of hybrid energies is indicated in Fig. 4. It is preferable in studying any

TABLE II. Parameters for the elements. ϵ_s and ϵ_p are the atomic term values obtained from (or extrapolated from) the Herman-Skillman tables (Ref. 8). V_1^a and V_1^c are the matrix elements of Eqs. (21) and (22). The ϵ_h^a and ϵ_h^c are hybrid energies chosen to reproduce approximately the polar energies using the relation $V_3 = (\epsilon_h^c - \epsilon_h^a)/2$.

Element	$-\epsilon_s$ (eV)	$-\epsilon_p$ (eV)	$V_1^{c,a}$ (eV)	$-\epsilon_h^{c,a}$ (eV)
Be	8.17	4.14	1.01	6.27
B	12.54	6.64	1.47	6.18
C	17.52	8.97	2.13	~7.65
N	23.04	11.47	2.88	10.10
O	29.14	14.13	3.76	10.58
F	35.80	16.99	4.71	14.66
Mg	6.86	2.99	0.97	3.88
Al	10.11	4.86	1.33	4.74
Si	13.55	6.52	1.76	~5.70
P	17.10	8.33	2.19	7.10
S	20.80	10.27	2.63	8.12
Cl	24.63	12.31	3.08	8.70
Cu	6.92	1.83	1.27	3.76
Zn	8.40	3.38	1.25	3.48
Ga	11.37	4.90	1.62	4.44
Ge	14.38	6.36	2.00	~5.80
As	17.33	7.91	2.36	6.86
Se	20.32	9.53	2.70	8.00
Br	23.35	11.20	3.02	9.30
Ag	6.41	2.05	1.09	3.34
Cd	7.70	3.38	1.08	3.30
In	10.12	4.69	1.36	4.28
α-Sn	12.50	5.94	1.64	~5.30
Sb	14.80	7.24	1.89	6.47
Te	17.11	8.59	2.13	7.46
I	19.42	9.97	2.36	8.64
Hg	7.68	3.36	1.08	~3.10

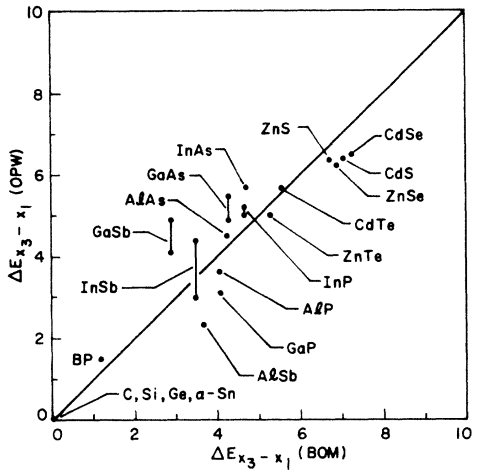

FIG. 5. Principal valence-band splitting at X plotted against the BOM calculations using the parameters of Table I. The line corresponds to $\beta = 0.8$ in Eqs. (21) and (22). Values were obtained from band calculations of Herman and co-workers. All values are in eV.

property to use the V_3 value from Table I, but the hybrid energies provide an estimate if V_3 is not known and will be of interest in their own right when we consider photoelectric thresholds.

The determination of V_1 values was a considerably different problem. The quantities entering the calculations of bands are of the form $A = M_1^a u_a^2$ and $C = M_2^c u_c^2$. The crudeness of the resulting bands suggested that the use of the complex formulas, Eqs. (13) and (14), was not justified. Use of the approximate forms $\frac{1}{2}M_1^a(1+\alpha_p)$ and $\frac{1}{2}M_1^c(1-\alpha_p)$ and values of M_1^a and M_1^c from the Herman-Skillman tables led to principal valence-band gaps which were 20% too large on the average. It seemed appropriate to conclude that on the average the s-p splitting in the solid is less than that in the atom and scale the values of V_1. We therefore took

$$V_1^a = \beta(\epsilon_p^a - \epsilon_s^a)/2, \tag{21}$$

$$V_1^c = \beta(\epsilon_p^c - \epsilon_s^c)/2, \tag{22}$$

with $\beta = 0.8$, and used term values from the Herman-Skillman tables.[8] We also use the simplified expressions

$$A = \tfrac{1}{2} V_1^a (1+\alpha_p), \tag{23}$$

$$C = \tfrac{1}{2} V_1^c (1-\alpha_p). \tag{24}$$

A comparison of the results with full band calculations appears in Figs. 5 and 6. The correlation is indeed very good and the same value $\beta = 0.8$ appears appropriate in both cases. In making a choice for β we absorb not only corrections to the matrix element M_1, but also corrections to u_a^2 and u_c^2 from S. The average value, which we call the *metallic energy*,

$$V_1 = A + C \tag{25}$$

is listed for each compound in Table I. The values for the individual elements are given in Table II.

The variation of parameters, particularly the covalent energy, with volume plays an important role in the model. We have not, as in I, used the bond length in determining V_2; we have instead established values for C, Si, Ge, and Sn from absorption peaks, assumed compounds from two elements of the same row with one of these will have the same covalent energy (e.g., V_2 for GaAs the same as that for Ge), and taken a geometric mean for skew compounds. However, the bond length increases monotonically with row in the Periodic Table, is about the same for compounds made of elements from a single row, and is intermediate for skew compounds. Thus the covalent energy *will* be a monotonic function of d. In Fig. 7 we have plotted $\ln V_2$ against $\ln d$ for C, SiC, Si, Ge, and Sn (compounds fall on the same line). We see that the covalent energy varies as d^{-2}, not as d^{-3} as found in the earlier determination of parameters. This is indeed a plausible result. The pseudopotentials for Si, Ge, and Sn, normalized to the free-electron Fermi energy, are almost the same functions of $q/2k_F$.[11] To the extent they are the same, the bands and all band gaps would scale precisely with d^{-2}. The ultimate origin of this tendency may well come from the virial theorem with its scaling of kinetic and potential energies.[12]

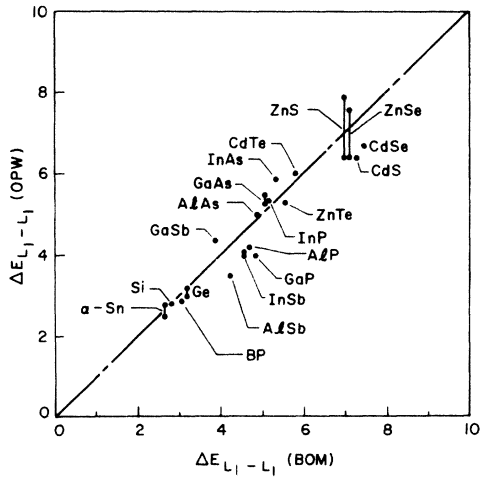

FIG. 6. Principal valence-band splitting at L plotted against the BOM calculations using the parameters of Table I. The dashed line corresponds to $\beta = 0.8$ in Eqs. (21) and (22). Values were obtained from band calculations of Herman and co-workers. All values are in eV.

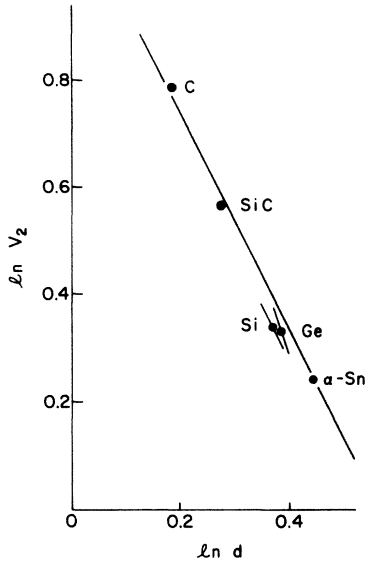

FIG. 7. Logarithm of the covalent energy versus the logarithm of bond length. The straight line corresponds to V_2 proportional to d^{-2}. The lines through Si and Ge represent the experimental variation of V_2 with pressure.

We cannot, of course, deduce that the covalent energy will follow the same curve when d is changed for a given material under pressure. However, to some extent the pseudopotential, normalized as above, is rather insensitive to pressure[13] so it is a reasonable possibility. Fortunately the variation of the principal absorption peak E_2 with pressure has been measured by Zallen and Paul.[14] They give a value of

$$s = \frac{-d}{E_2}\frac{\partial E_2}{\partial d} \tag{26}$$

[which equals $-(d/V_2)\,\partial V_2/\partial d$ for nonpolar systems] of 2.0 for Si and 3.2 for Ge. These are indicated also in Fig. 7. The precision of such measurements is not high and it is reasonable to proceed with a universal value of $s = 2.0$ for column-four semiconductors.

We may also expect the polar energy to vary with volume. Physically, V_3 contains a difference in atomic energies but also a Madelung energy which increases with decreasing d. Thus we expect V_3 also to increase as d decreases. Measurements by Zallen and Paul[14] on GaSb ($s = 2.1$) and InSb ($s = 1.7$) are consistent with a dependence of V_3 on d similar to that of V_2, but the information is not very conclusive.

Further information about the volume dependence is obtainable from the pressure dependence of the dielectric constants. For nonpolar materials ϵ_0 depends upon d through the factors N, d^2, and V_2^{-1}, assuming that γ is independent of volume. We obtain immediately

$$\frac{d}{\epsilon_0 - 1}\frac{\partial(\epsilon_0 - 1)}{\partial d} = -1 + s, \tag{27}$$

which is unity for $s = 2$. Recent measurements by Biegelsen[15] give 0.74, in reasonable agreement with the prediction of unity. Earlier measurements on Ge by Abrams and Pinnow[16] give the very large value of 12, for reasons we do not understand.

Variations in the parameters when one ion moves with respect to its neighbors are also of considerable interest. There are important differences from the case of uniform compression. We may expect the matrix element between two hybrids, represented by M_2, and the overlap S in each bond to shift with bond length the same way in both cases, and therefore V_2 should have the same dependence on d. However, we expect no change in V_3 linear in the change in d; the Madelung energy must by symmetry be quadratic in displacements of a single ion. The change in V_2 linear in displacement gives rise to a subtle effect when we seek the induced dipole due to such a displacement; the point has been carefully discussed by Martin.[17] If we displace an ion the polarity of the bonds in front of that ion is decreased (as V_2 increases) while the polarity of those behind is increased (as V_2 decreases). The net charge on the ion is unchanged to first order in the displacements (just as V_3 is unchanged to first order) but the charge transfers add up and contribute to the bulk polarization. (For long-wavelength spacially varying polarizations this leads to accumulation in the bulk; for uniform polarizations in finite systems it leads to surface charges.) Such extra contributions are absolutely essential to the understanding of effective charges to be discussed in Sec. IV.

IV. CALCULATED PROPERTIES

We have already discussed a number of properties while establishing the parameters. Our purpose here is to further test our choice using a variety of properties. This comparison is considerably more extensive than the illustrative examples given in I but is not exhaustive. More complete studies aimed at understanding the properties in question (rather than testing the model) are in order. Such a study of the valence bands themselves is being prepared separately.[18] In addition, studies of quite different properties, such as states arising at semiconductor surfaces,[19] can be most informative.

A. Valence bands

The energy bands of gallium arsenide from the best available band calculation were shown in Fig.

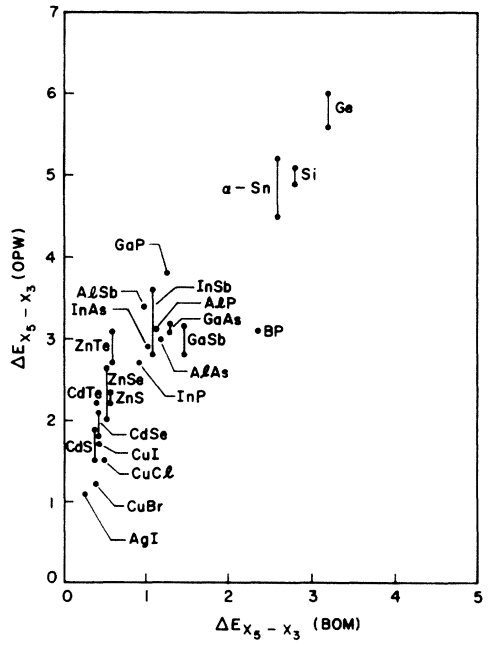

FIG. 8. Secondary valence-band splitting at X plotted against the predictions of the bond-orbital model using the parameters of Table I. Band calculations were by Herman and co-workers. All values are in eV.

1 for the [100] and [111] directions. Various symmetry points in the valence bands are indicated and we will use the same notation for elemental semiconductors though in that case some of the gaps must vanish by symmetry and different notation is customary. We saw in I that in the bond-orbital model the two upper bands are found to be completely flat. The distortion of these bands, which is apparent on the left in Fig. 1, could only be obtained by the inclusion of more distant neighbor overlaps or the distortion of the basis states themselves. We regarded the gaps X_3-X_1 and L_1-L_1 as the principal gaps and have already in Figs. 5 and 6 plotted the best available values from band calculations against our prediction. Other features of the band structure are not so well given. In most cases the true values are monotonic functions of our predicted values, as illustrated in Figs. 8 and 9. At the same time the bond-orbital model yields significant trends (both with polarity and metallicity) of the bandwidth Γ_{15}-Γ_1, while full band calculations show that they are rather constant. In other cases (for example, Γ_{15}-X_5) our prediction is zero. Even these shifts, which are not present in the crudest form of the theory, *do* correlate with the parameters of the model and it is possible to use the model as an interpolation scheme to predict the energies at symmetry points for all tetrahedral semiconductors and to understand in terms of the model various trends among the band structures.[18] Both of these discussions are beyond the scope of the present article.

Very recently Shevchik, Tejeda, and Cardona[20] have shown that the addition of second-neighbor matrix elements removes the principal discrepancies in these bands. Indeed by adding still further overlaps we can presumably reproduce exactly the observed bands. Most importantly, even with the addition of these matrix elements, the diagonalization of the 4×4 matrix to obtain the valence bands is a unitary transformation which leaves the total charge density and the total energy unchanged. The calculation of all of the other properties we consider is therefore unaffected and is at the same time consistent with as accurate a description of the bands as one has the patience to provide. The refinement of the bands and the calculation of other properties are quite separate problems.

B. Effective ionic charge

There are essential ambiguities in associating effective charges with ions, ultimately coming from the fact that in a periodic structure there are innumerable reasonable ways to divide up the charge. In the context of the bond-orbital model the natural choice is to associate a fraction $\frac{1}{2}(1+\alpha_p)$ of the two electronic charges per bond with the

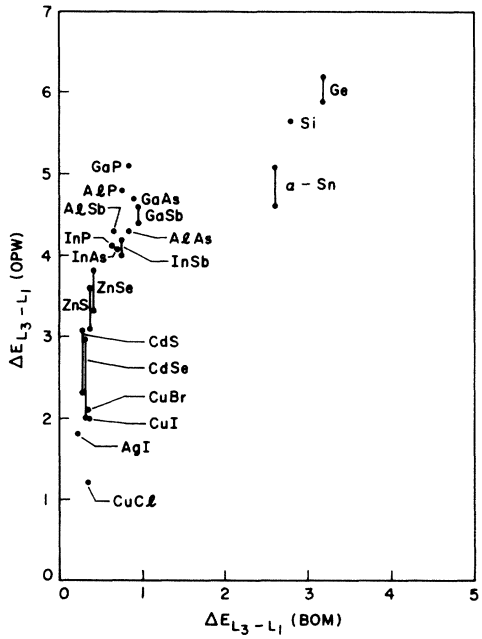

FIG. 9. Secondary valence-band splitting at L plotted against the predictions of the bond-orbital model using the parameters of Table I. Band calculations were by Herman and co-workers. All values are in eV.

anion and a fraction $\frac{1}{2}(1-\alpha_p)$ with the cation. This leads to an effective ionic charge of magnitude (in electron charges)

$$Z^* = 4\alpha_p - \Delta Z \ , \tag{28}$$

where ΔZ is 1 for III-V compounds, 2 for II-VI compounds, and 3 for I-VII compounds. It is striking that the first term almost always dominates and Z^* tends to decrease with increasing ΔZ. However, this definition is somewhat arbitrary and it makes more sense to define a charge which, at least in principle, is measurable.

C. Transverse charge

Perhaps the most physical definition for tetrahedrally coordinated solids is the macroscopic transverse effective charge e_T^*. It could be defined by displacing every anion by a small distance $\vec{\delta}$ with respect to every cation, measuring the surface charge required to neutralize the resulting volume dipole, and equating e_T^* to the point charge which would cause such a dipole. In a zinc-blende structure the result does not depend upon the direction displaced. It is most conveniently calculated by using displacements in a [100] direction so all bonds are equivalent.

In I we distinguished two contributions, one which would occur if α_p did not change with bond length, and a second due to the change in α_p. The first we correctly identified with the Z^* of Eq. (28). Note that no factor γ could appear since as α_p approaches 1 the result must be $4-\Delta Z$. If we made this evaluation in terms of changes in dipole for each bond, using Eq. (18), we would conclude that γ must change with such distortions. The second contribution can be seen by moving a metallic ion to the right (positive x direction) and considering the bond to a neighboring nonmetallic ion to the left. The change in bond length is $\delta/\sqrt{3}$ causing a change in α_p of $s\alpha_p\ (1-\alpha_p^2)\ \delta/\sqrt{3}d$ [using Eq. (26)] and therefore a dipole change in the x direction of $\gamma e s\alpha_p(1-\alpha_p^2)\ \delta/3$. The contributions of the four bonds add to give a total dipole per ion the same as would be produced by a charge of

$$e_T^* = Z^* + 4\gamma s\alpha_p(1-\alpha_p^2)/3 \tag{29}$$

protons moving with the ion. If s is replaced by 3 this becomes the result obtained in I. Here we take $s=2$ and obtain the transverse charges which are compared with experiment in Fig. 10. The model reproduces the large effective charges and the rather weak trend with polarity though the predictions could hardly be called accurate. It should be remembered that the input parameters are obtained from quite unrelated properties.

An independent study of e_T^* made by Lannoo and Decarpigny[5] was conceptually equivalent to this discussion though they sought parameters in a much different way. Indeed there is a one-to-one correspondence between their parameters and ours. Their $\alpha_B - \alpha_A$ is equivalent to our $2V_3$; their β is equal to our V_2; their q_A is our Z^*; and their f, which they call the ionicity parameter, is related through the dielectric constant to polarity by $f = [1 - (1-\alpha_p^2)^{3/2}]^{1/2}$.

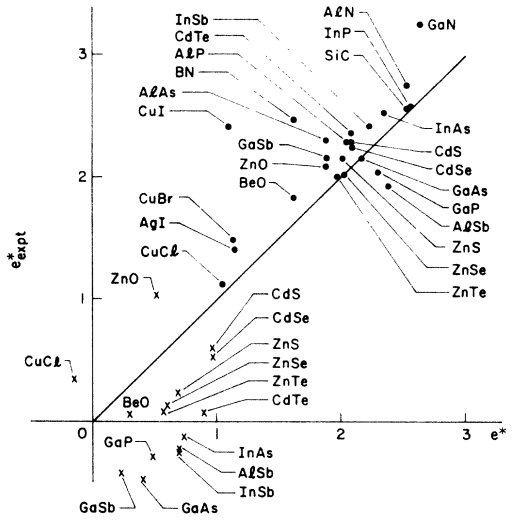

FIG. 10. Experimental macroscopic transverse charges (compiled by Lucovsky *et al.*, Ref. 21) (points) plotted against the predictions of Eq. (29) and experimental piezoelectric charges (compiled by Martin, Ref. 17) (crosses) plotted against the predictions of Eq. (33).

D. Piezoelectric effect

The piezoelectric effect allows a second and physically different definition of a measurable effective charge. We introduce a shear strain and find that the two ions in each primitive cell are displaced with respect to each other. If we know the displacements and measure the polarization density we may define an effective charge e_p^*, which would equal Z^* (just as would the macroscopic transverse charge) if α_p did not change. We will see that the contributions from the charge transfer are of opposite sign in this case to those for e_T^*.

We introduce a pure shear strain

$$S_4 = \frac{\partial u_y}{\partial z} + \frac{\partial u_x}{\partial y} \tag{30}$$

by introducing displacements $u_y = S_4 z/2$ and $u_x = S_4 y/2$. This will give rise to internal displacements of the anion sublattice with respect to the cation sublattice *in the x direction* of

$$\delta u_x = \zeta a S_4/4 \ , \tag{31}$$

where ζ is Kleinman's[22] internal displacement parameter, which has been calculated by Martin[17] by

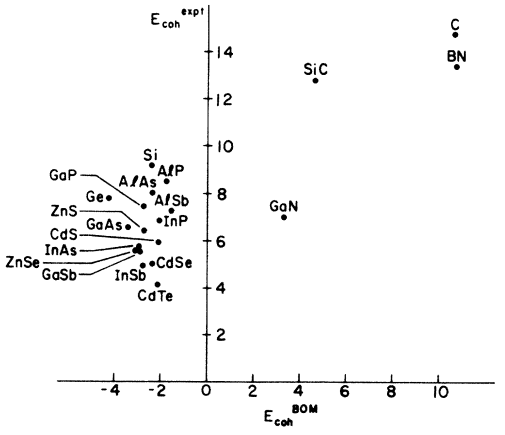

FIG. 11. Experimental cohesive energy in eV plotted against the bond-orbital model result which does not include overlap energy nor correlation energy. Experimental values taken from C. Kittel, *Introduction to Solid State Physics* (Wiley, New York, 1971), and N. N. Sirato, *Semiconductors and Semimetals* edited by R. K. Willardson and A. C. Beer (Academic, New York, 1968), Vol. 4.

fitting force constants to the observed elastic constants. It was defined so that it would equal 1 if all bond lengths remain the same under a pure shear. We may directly compute the change in bond length for each bond surrounding an anion:

$$\delta d/d = \pm S_4(1-\zeta)/3 \,. \tag{32}$$

The changes in the x components of the dipoles from four bonds surrounding a given anion are all equal and subtract from the contribution of the direct anion displacement. This leads to an effective charge for piezoelectricity given by

$$e_p^* = Z^* - 4\gamma s\alpha_p(1-\alpha_p^2)\,(1-\zeta)/3\zeta \,. \tag{33}$$

This charge is related to the piezoelectric constant by $e_{14} = e_p^* \zeta e/a^2$. We have plotted the observed[17] effective charges against those from Eq. (33) also on Fig. 10. Again the scatter is quite large but the significant difference between observed e_T^* and e_p^* is reproduced. This is indeed a sensitive test of the bond-orbital model since not only is there extensive cancellation between the two terms in Eq. (33), but ζ is near 1 (between 0.64 and 0.90) and our predictions are therefore very sensitive to this uncertain parameter.

E. Cohesive energy

The cohesive energy is obtained by moving step by step from isolated neutral atoms to the solid, obtaining the change in energy with each step. Here we imagine promoting the electrons to hybrid states in each isolated atom (requiring an energy E_{pro}) and then bringing the atoms, with frozen wave functions, together as a solid. The only energy change in this second step is the change in Coulomb energy of the overlapping charge densities. This *overlap energy*, which was not considered in I, is increasingly negative as the atoms are brought together, reaches a minimum, and then increases as the ion cores near each other. The overlap energy is presumably important in setting the atomic spacing but may be less important in the total energy. We may expect it to depend upon the equilibrium bond length d, but not to depend sensitively on polarity.

In the next step we form bonds, as in I, and obtain the same result [Eq. (31) in I] with an additional term $-8V_2S$ [see Eq. (11) here] and of course use slightly different parameters. Finally we should note[12] that there is an interbond, or interatomic, correlation energy which would appear not to have been included in the parameters V_2 and V_3, since they only reflect changes in energy as the wave functions are modified.

Since the correlation energy and overlap energy are uncertain at this stage we may first compute the remaining terms, as in I, to obtain

$$E_{coh}^{BOM} = 8(V_2^2+V_3^2)^{1/2} - 8SV_2 - 2\Delta Z V_3 - E_{pro} \tag{34}$$

per atom pair. (The term $-8SV_2$ did not appear in I.) The observed cohesive energy is plotted against this in Fig. 11. At first glance this would appear a disaster; the new term $-8SV_2$ has made most values negative. However the *trend* with V_2 (see C, SiC, Si, Ge) is approximately correct, whereas the variation was seriously overestimated in I. Further, the deviations from experiment appear to systematically decrease with polarity. This suggests correlation energies may be the most im-

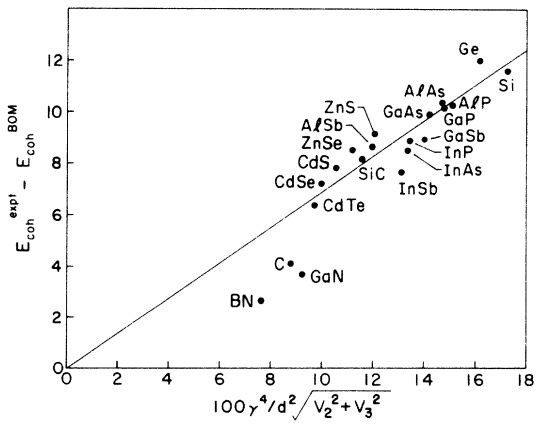

FIG. 12. Discrepancy between experimental cohesive energy and the bond-orbital result plotted against a form of contribution motivated by consideration of the interbond correlation energy.

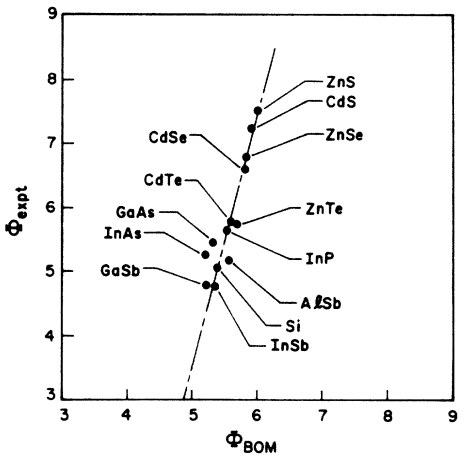

FIG. 13. Experimental photoelectric threshold in eV plotted against the BOM prediction of Eq. (38). Experimental values taken from R. Swank, Phys. Rev. 153, 884 (1967), G. W. Gobeli and F. G. Allen, Phys. Rev. 127, 141 (1962); 127, 150 (1962); 137, A245 (1965); and T. E. Fisher, Phys. Rev. 129, A1228 (1965); 142, 519 (1966).

portant terms omitted and it is of interest to look at these more carefully.

We have constructed one-electron energies in terms of individual bonds. These bonds, however, are polarizable and there will be van der Waals interactions between them which go beyond this one-electron approximation. We may estimate this interaction but must recognize that there is also correlation energy within separated atoms and only some of the difference is hidden in V_2 and V_3. Thus at best we can only hope for a qualitative form of correction to the cohesive energy.

The dielectric constant of Eq. (20) corresponds to a dipole matrix element between bonding and antibonding states in each bond of

$$\langle a|x|b\rangle \propto \gamma d(1-\alpha_p^2)^{1/2} . \tag{35}$$

For two bonds separated by r, the matrix element of the electron-electron interaction between the ground state and the state with one electron from each bond in an antibonding state is proportional to $\gamma^2 e^2 d^2(1-\alpha_p^2)/r^3$. The van der Waals interaction, or correlation energy, is the lowering in energy to second order in this matrix element,

$$E_{cor} \propto \frac{\gamma^4 e^4 d^4 (1-\alpha_p^2)^2}{r^6 (V_2^2+V_3^2)^{1/2}} \propto \frac{\gamma^4 e^4 (1-\alpha_p^2)^{5/2}}{d^2 V_2} . \tag{36}$$

Any estimate of the magnitude of the energy from Eq. (36) gives much too large a value, indicating self-consistent screening is needed. Division by ϵ_0^2 on the other hand gives too small a value, so the problem is intermediate and difficult.

Because V_2 varies roughly as d^{-2}, Eq. (36) gives a result independent of bond length, in accord with the discrepancies from Fig. 11. On the other hand, the dependence upon α_p in Eq. (36) is too strong, perhaps because screening is larger when α_p is small. The best account of the cohesion is obtained when $(1-\alpha_p^2)^{5/2}$ is replaced by $(1-\alpha_p^2)^{1/2}$, as suggested in Fig. 12. This leads us to a semiempirical expression for the correlation (and overlap) energies and a total cohesive energy of

$$E_{coh} = E_{BOM} + 0.33\gamma^4 e^4/d^2(V_2^2+V_3^2)^{1/2} , \tag{37}$$

with E_{BOM} given in Eq. (34). This can of course not be regarded as a prediction of the theory but a semiempirical formula, with plausible motivation, and with the very good correlation with experiment suggested by Fig. 12.

F. Photoelectric threshold

Because we have hybrid energies, measured from the vacuum, and band energies relative to the hybrid energies, we may directly write an expression for the top of the valence band relative to the vacuum. This is the photoelectric threshold,

$$\phi_{BOM} = \tfrac{1}{2}|\epsilon_h^a + \epsilon_h^c| + (V_2^2+V_3^2)^{1/2} - SV_2 - V_1 . \tag{38}$$

This value is subject to the same omissions as was the cohesive energy, and in addition omits contributions from surface dipoles. Thus we do not expect it to agree well with experiment. However, the plot in Fig. 13 of the experimental values against Eq. (38) shows at least a good linear correlation. A line such as that drawn could be used as an empirical formula though Eq. (38) itself is very inaccurate.

†Supported in part by National Science Foundation under Grant GP 25945 and in part by the National Science Foundation through the Center for Materials Research at Stanford.

*On leave of absence from the Middle East Technical University Ankara, Turkey.

[1]G. G. Hall, Philos. Mag. 43, 338 (1952).
[2]C. A. Coulson, L. R. Redei, and D. Stocker, Proc. R. Soc. Lond. 270, 357 (1962).
[3]G. Lehman and J. Friedel, J. Appl. Phys. 33, 281 (1962).
[4]G. D. Watkins and R. P. Messmer, in *Computational Methods for Large Molecules and Localized States in Solids*, edited by F. Herman, A. D. McLean, and R. K. Nesbet (Plenum, New York, 1973), p. 133.
[5]M. Lannoo and J. N. Decarpigny, Phys. Rev. B 8, 5704 (1973).
[6]J. C. Phillips, *Bonds and Bands in Semiconductors* (Academic, New York, 1973).
[7]W. A. Harrison, Phys. Rev. B 8, 4487 (1973).
[8]F. Herman and S. Skillman, *Atomic Structure Calculations* (Prentice Hall, Englewood Cliffs, N.J., 1963).

[9]S. Ciraci, Ph.D. thesis (Stanford University, 1974) (unpublished).
[10]J. C. Phillips, Ref. 6, p. 169.
[11]See, for example, W. A. Harrison, *Pseudopotentials in the Theory of Metals* (Benjamin, New York, 1966), p. 314.
[12]J. J. Hopfield (private communication).
[13]Reference 11, p. 58.
[14]R. Zallen and W. Paul, Phys. Rev. 155, 703 (1967).
[15]David K. Biegelsen (unpublished).
[16]R. L. Abrams and P. A. Pinnow, J. Appl. Phys. 41, 2765 (1970).
[17]Richard M. Martin, Phys. Rev. B 5, 1607 (1972), and private communication.
[18]S. Ciraci and S. T. Pantelides (unpublished).
[19]S. Ciraci, W. A. Harrison, Paul Gregory, W. E. Spicer, and L. F. Wagner, Bull, Am. Phys. Soc. II 19, 214 (1974).
[20]N. J. Shevchik, J. Tejeda, and M. Cardona, Phys. Rev. B 9, 2627 (1974).
[21]G. Lucovsky, R. M. Martin, and E. Burstein, Phys. Rev. B 4, 1367 (1971).
[22]L. Kleinman, Phys. Rev. 128, 2614 (1962).